



COMPRESSIVE SENSING BASED CHANNEL ESTIMATOR AND LDPC THEORY FOR OFDM USING SDR

ESTIMADOR DE CANAL BASADO EN SENSADO COMPRESIVO Y LDPC PARA OFDM USANDO SDR

Anthony Yanza-Verdugo¹, Christian Pucha-Cabrera¹ and Juan Inga-Ortega^{2,*}

Abstract

This work proposes the application of a channel estimator based on Compressive Sensing (CS) on a system that employs Orthogonal Frequency Division Multiplexing (OFDM), utilizing Software Defined Radio (SDR) devices. The application of the CS theory is given through the use of sparse reconstruction algorithms such as Orthogonal Matching Pursuit (OMP) and Compressive Sampling Matching Pursuit (CoSaMP), in order to take advantage of the sparse nature of the pilot subcarriers used in OFDM, optimizing the bandwidth of system. In addition, to improve the performance of these algorithms, the concept of sparse parity checking matrix is used, which is implemented in the deployment of low density parity check codes (LDPC) to obtain a sensing matrix that improves the isometric restriction property (IRP) belonging to the CS paradigm. The document shows the model implemented in the SDR equipment, analyzing the bit error rate and the number of pilot symbols used.

Keywords: Channel Estimation, LDPC, OFDM, SDR, Compressive Sensing.

Resumen

Este trabajo propone la aplicación de un estimador de canal basado en sensado compresivo (CS, del inglés *Compressive Sensing*) sobre un sistema que usa multiplexación por división de frecuencias ortogonales (OFDM, del inglés *Orthogonal Frequency Division Multiplexing*) usando dispositivos de radio definido por *software* (SDR, del inglés *Software Defined Radio*). La aplicación de la teoría de CS se da a través del uso de algoritmos de reconstrucción dispersa como *Orthogonal Matching Pursuit* (OMP) y *Compressive Sampling Matching Pursuit* (CoSaMP) con el fin de aprovechar la naturaleza dispersa de las subportadoras piloto usadas en OFDM optimizando el ancho de banda del sistema. Además, para mejorar el rendimiento de estos algoritmos, se utiliza el concepto de la matriz de comprobación de paridad dispersa que se implementa en el despliegue de códigos de comprobación de paridad de baja densidad (LDPC, del inglés *Low Density Parity Check*) para obtener una matriz de sensado que mejore la propiedad de restricción isométrica (RIP, del inglés *Isometric Restriction Property*) perteneciente al paradigma de CS. El documento muestra el modelo implementado en los equipos SDR analizando la tasa de error de bit y la cantidad de símbolos piloto usados.

Palabras clave: estimación de canal, LDPC, OFDM, SDR, sensado compresivo.

^{1,*}Electronics Engineering / GITEL, Universidad Politécnica Salesiana – Ecuador.

¹ <http://orcid.org/0000-0002-1710-3052>, ² <http://orcid.org/0000-0002-4734-7218>

²Telecommunications / GITEL, Universidad Politécnica Salesiana – Ecuador.

Correspondence author ✉: jinga@ups.edu.ec ² <http://orcid.org/0000-0003-2580-9677>

Received: 31-10-2019, accepted after review: 09-12-2019

Suggested citation: Yanza-Verdugo, A.; Pucha-Cabrera, C. and Inga-Ortega, J. (2020). «Compressive Sensing Based Channel Estimator and LDPC Theory for OFDM using SDR». INGENIUS. N.º 23, (january-june). pp. . DOI: <https://doi.org/10.17163/ings.n23.2020.07>.

1. Introduction

The orthogonal frequency division multiplexing (OFDM) is currently the transmission technique mostly implemented in wireless networks, due to its advantages in high speed data transmission through frequency selective channels. Thereby, the use of OFDM has had a high performance because of its high efficiency in the use of the radio spectrum and its robustness to multipath delay [1, 2]. In addition, the inter symbol interference (ISI) and inter carrier interference (ICI) are reduced through the use of a cyclic prefix, enabling the replacement of complex time-domain equalizers by a simple frequency-domain equalizer [3]. In this sense, for frequency selective and time-varying radio channels in broadband mobile communication systems, it is necessary to apply a reliable channel estimation to implement coherent detection [1].

There are three types of channel estimators: blind estimation, semi-blind estimation and pilot symbol assisted modulation (PSAM). PSAM uses pilot symbols that are known by both receiver and transmitter at different positions, to obtain an approximation of the channel in exchange for losing spectral efficiency. On the other hand, blind estimation is focused on statistical processes with high mathematical level exhibiting improvements regarding spectral efficiency, even though it is not commonly used nowadays due to its high complexity, slow speed of convergence and low performance [4]. At last, the semi-blind estimation combines the two previous approaches to yield a compromise between complexity and efficiency; for this matter, both training sequences and statistical models of the channel are utilized [5].

On the basis of the above, this work proposes the use of PSAM for channel estimation, where the gain of the channel and the phase distortion are obtained from the received signal at the positions of the pilot symbols [1]. These pilot symbols are also utilized to improve the synchronization of time and frequency in the communication system. Nevertheless, it is necessary to use a greater percentage of pilot symbols to increase the performance, which implies that certain subcarriers do not transmit information [2].

In addition, in this work the number of pilot subcarriers is reduced through the use of compressive sensing (CS) in the estimation of the channel, in order to improve the utilization of the bandwidth. This can be applied since it is possible to estimate the channel taking advantage of the CS theory, considering that the number of pilot symbols is sparse with respect to the total number of symbols that constitute an OFDM message, thus obtaining a compressed version of the channel corresponding to its effects on the pilot subcarriers [6].

The process is also optimized for implementation on software defined radio (SDR) equipment, through

the use of the low density parity check (LDPC) matrix in combination with the CS paradigm.

The rest of the paper is organized as follows. Section 2 discusses the mathematical modeling of OFDM, CS and the application of LDPC matrices with CS. Section 3 describes the implementation in the SDR devices using LDPC matrices with CS. Section 4 presents the results obtained, and the analysis of the bandwidth and the bit error rate (BER). At last, section 5 gives the conclusions and recommendations for future works.

2. Mathematical modeling

The implementation is developed from the mathematical model of OFDM, where an OFDM symbol is represented by $S(q) \in \mathbb{R}^Q$, such that a set of Q information symbols is transmitted by symbol j of OFDM; each with a subcarrier q is denoted as $S_j(q)$, thus that $[S_j(0), \dots, S_j(q), \dots, S_j(Q-1)]^T$ represents the vector of information symbols transmitted in the j -th OFDM symbol [2, 7].

Each OFDM symbol uses the serial flow of information symbols, converting them into Q parallel flows and later inserting the pilot symbols necessary in the estimation of the channel according to the proposed transmission scheme. Besides, subcarriers in zero are added to establish guard bands between each OFDM symbol, thus avoiding the interference of adjacent channels. The number of subcarriers of an OFDM symbol is given by

$$Q = I + P + Z \quad (1)$$

where I corresponds to the number of subcarriers with information, P is the number of pilot subcarriers and Z is the number of subcarriers in zero, for an OFDM symbol. According to this, equation (2) describes the format of an OFDM symbol corresponding to the frequency domain, and then the inverse discrete Fourier transform is applied to obtain the symbol in the time domain, as described in equation (3). The distribution of the zero-padding is detailed in [8].

$$S_z(q) \triangleq \begin{cases} S(q), & \frac{Q-(I+P)}{2} \leq q \leq \frac{Q-(I+P)}{2} - 1 \\ 0, & \text{any other case} \end{cases} \quad (2)$$

$$S_z = F^H S \quad (3)$$

The reduction of ISI and ICI is due to the use of the so-called cyclic prefix (CP), which consists of a cyclic extension of the OFDM symbol. The CP is as long as the expected propagation delay, and the effects of both are found in [9]. On the other hand, the signal received for OFDM may be described in equation (4).

$$y_j = H_j s_j + z_j \quad (4)$$

The vector of received information symbols is $y_j = [y_j(0), \dots, y_j(Q-1)]^T$ in the j -th OFDM symbol, z_j is the Gaussian noise and H_j denotes the value of the channel for the j -th OFDM symbol, which is obtained by means of the channel estimation block [7].

The receiver uses the Van de Beek algorithm, which takes advantage of the cyclic prefix to establish the beginning and the end of an OFDM symbol. This algorithm will also allow correcting the effects of the channel in possible phase shifts, and avoid losing the orthogonality in the subcarriers [10].

In the following the cyclic prefix is removed and the discrete Fourier transform (DFT) is applied to recover the information symbols. Prior to the recovery of the information symbols, the channel is estimated after removing the zero-padding and extracting the pilot symbols. The equalized data are obtained through the operation indicated in equation (5) [11], where $\hat{H}_e(q)$ is the estimated channel. Table 1 presents a list of all the variables used along this work.

$$S_e = \frac{Y(q)}{\hat{H}_e(q)} \quad q = 0, 1, \dots, Q-1 \quad (5)$$

2.1. Compressive sensing

From another perspective, the CS paradigm considers a «sparse» signal x that possesses only K elements different than zero, with $K \ll N$ and where $x \in \mathbb{R}^N$. Then, through a matrix Φ of dimension $M \times N$, with $N > M$, known as sensing matrix, it is sought to concentrate the more relevant information in x through the use of another vector $y \in \mathbb{R}^M$. If this is not fulfilled, the ability of reconstructing x from y is reduced; this restriction is known as null space property (NSP) [11, 12].

It is not easy to find signals considered «sparse», however, it is possible to find an approximation to this concept which appears when the signal x may be «compressible» in some vector basis different to the original [11–13]. Therefore, $x = \Psi\alpha$, where Ψ (also called dictionary matrix of x) corresponds to the vector basis in which x is projected, and α corresponds to the atoms of x inside of the domain of Ψ . Thereby, the original signal may be represented through the linear combination proposed in (6) [14]. For instance, the dictionary may be of Fourier, DCT or Wavelet [11, 15, 16].

$$x = \Psi\alpha = \sum_{i=1}^N \alpha_i \psi_i \quad (6)$$

The compression of the signal x in the signal y may be obtained through (7), where $\Theta = \Phi\Psi$. Figures 1(a) and 1(b) graphically show the concept of CS [13, 17].

$$y = \Phi x = \Phi\Psi\alpha = \Theta\alpha \quad (7)$$

The literature suggests that Φ should be random to fulfill the isometric restriction property (IRP), and in this way x may be reconstructed from y [16, 18].

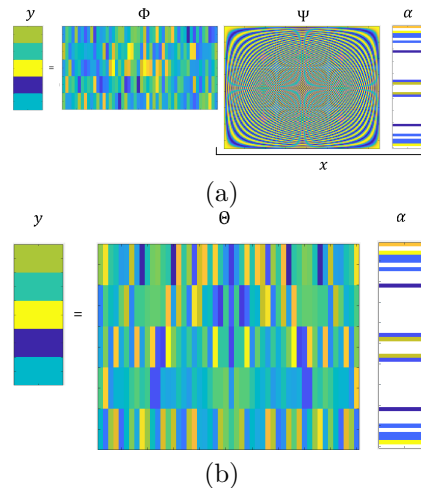


Figure 1. Principle of operation of compressive sensing: (a) measuring process in CS with random sensing matrix Φ and measuring matrix Ψ . (b) measuring process with $\Theta = \Phi\Psi$.

Table 1. List of variables

Variables	Description
Q	Total of subcarriers in the OFDM symbol.
$S_j(q)$	Subcarrier q in the j -th OFDM symbol.
I	Total of subcarriers with information.
P	Total of pilot subcarriers.
Z	Total of subcarriers in zero.
$S_z(q)$	OFDM symbol with zero-padding in subcarrier q .
F	Fourier transform matrix.
s_z	OFDM symbol with zero-padding in time.
y_j	Vector of received symbols in the j -th OFDM symbol in time.
H_j	Channel vector in the j -th OFDM symbol.
s_j	j -th OFDM symbol transmitted in time.
Z_j	Complex Gaussian noise.
$Y(q)$	OFDM symbol in frequency, after removing the cyclic prefix, zero-padding and without pilots.
S_e	Symbols equalized in frequency.
$H_e(q)$	Estimated channel in frequency.
x	Data vector of length N .
y	Compressed vector of length M .
Φ	Compressing or sensing matrix, Phi.
N	Total length of the vector of data to be compressed.
K	Total elements different than zero.
M	Total length of the vector of compressed data.
Ψ	Measuring or dictionary matrix, Psi.
α	Vector of sparse coefficients, alpha.
Θ	Sensing matrix in its complete form, Theta.
W_c	Number of logic "1"s per column in H_{LDPC}
W_r	Number of logic "1"s per row H_{LDPC}
H_{LDPC}	Parity matrix of LDPC.
A	Matrix of $D \times E$ elements.
B	Matrix of $D \times D$ elements.
D	Number of parity bits in the coding.
E	Number of information bits in the coding.
G	Total bits of information + parity (codeword).
H_l	Left side irregular parity matrix of LDPC.
SC	Right side staircase parity matrix of LDPC.
Tr	Right side triangle parity matrix of LDPC.
\hat{H}_p	Channel of pilots.
Y_p	Received pilot symbols.
S_p	Known pilot symbols.
N_f	Frequency separation between pilots.
Φ_{LDPC}	Sensing matrix constructed with LDPC base.

In general, the sensing matrices may be obtained from a random process with normal distribution, achieving a good performance during the reconstruction of the signal, even though these distributions may demand many resources [15, 16].

Since $N > M$ and $N \gg K$, the process of reconstructing x becomes the optimization problem formulated in equation (8), where it is sought to find the atoms α that minimize the error $\|y - \Theta\alpha\|_0$.

$$\alpha = \arg \min \|\alpha\|_0 \quad s.t. \Phi\Psi\alpha \quad (8)$$

Then, x may be reconstructed from α using equation (6). Nevertheless, the optimization problem has no solution since it is of type NP Hard [11–13]. In this respect, the sparse reconstruction algorithms seek to relax the optimization problem to obtain a pseudo-optimal solution. In addition, their performance can be improved if it is used an appropriate sensing matrix which enables preserving the information and guarantees the reconstruction of the original signal in a unique manner [15, 16, 19–22].

The Orthogonal Matching Pursuit (OMP) can be highlighted, among the most popular sparse reconstruction algorithms used in the application of CS for channel estimation. OMP belongs to the types of algorithms based in greedy search, thus it is based on successive approximations of the α coefficients, identifying the support of the signal in an iterative manner until the convergence criterion is reached [19, 23]. The OMP algorithm is described in Table 2.

Another algorithm of sparse reconstruction employed in this case of application of CS, is the Compressive Sampling Matching Pursuit (CoSaMP) described in [24]. The algorithm approximates the objective signal in an iterative manner, and in each iteration, the current approximation obtains a residual updating the samples such that they reflect the current residue. These samples are utilized to identify the large components, to estimate the approximation using least squares. This process is repeated until the recoverable energy of the signal is found. The CoSaMP algorithm is described in Table 3 [25].

These algorithms are suitable to be used in applications or reconstructions where they operate in real time, due to their low computational cost.

Since the sensing matrix should fulfill the isometric restriction property (IRP), the use of parity check matrices is considered in the design of channel coders in the LDPC codes, since they fulfill the IRP criterion and are deterministic; therefore they consume less resources, thus being a good choice for the measuring matrix in CS [20–22]. This will enable to avoid the use of a pattern of pilots of the comb or block types, as it is commonly utilized in OFDM with PSAM. On this basis, it is sought to use a sparse pseudorandom pattern of pilots employing an LDPC parity check

matrix [5].

Table 2. OMP algorithm

Algorithm 1: Algorithm OMP (Orthogonal Matching Pursuit)	
Step 1	Input: $Y = \{y_1, \dots, y_M\}$; Compressed Input $\Theta_{N,N}$: Complete sensing matrix k : Number of repetitions
Step 2	Output: α_N
Step 3	Initialization: $res_M = Y$; $indx = \phi$;
Step 4	for $iter = 1$ to k : $\lambda = \arg \max \Theta^T \times res_M$; $indx = indx \cup \lambda_M$; $\alpha_N = \phi$; $\alpha_N(indx) = pinv(\Theta(:, indx)) \times Y$; $res = Y - \Theta \times \alpha_N$; endfor
Step 5	Return: α_N

Table 3. CoSaMP Algorithm

Algorithm 2: Algorithm CoSaMP (Compressive Sampling Matching Pursuit)	
Step 1	Input: $x \in R^N$; Compressed Input $\Theta \in R^{m \times N}$; $\text{con } N > m$; Complete sensing matrix k : Number of repetitions
Step 2	Output: S_{est}
Step 3	Initialization: $u = \Theta x$, Measuring vector; $\Omega = \{1, 2, \dots, N\}$ Column index of Θ ;
Step 4	for $iter = 1$ to k : $\Omega_k \subset \Omega \rightarrow \Theta_{\Omega_k}$; $\Omega_{k+1} = J_s^*$ where $J_s^* \subset \Omega$; $J = \text{Supp}\{T_1(\Theta \times r_k ; \tau_{k,1})\}$ with $ J \leq 2s$; where: T_1 is a threshold function such that: $\tau_{k,1} \geq 0$; τ_k : residual; with $\Omega_k \cup J$: $\ u - \Theta I_{\Omega_k \cup J} b\ _2$ minimized; where: $I_{\Omega_k \cup J}$ is an $N \times N$ diagonal matrix; $i \in \Omega_k \cup J$; $J_s^* = \text{Supp}\{T_2(b ; \tau_{k,2})\}$; where: T_2 is a threshold function; $\tau_{k,2} \geq 0$ maximum of s elements of b that are retained; $S_{est} = b(J_s^*)$; $r_{k+1} = u - \Theta I_{\Omega_{k+1}} b$; endfor
Step 5	Return: S_{est}

2.2. LDPC Parity check matrix

The parity check matrix H_{LDPC} defines the relationships between the different codification symbols (source symbols and parity symbols). There are two types, the regular matrices which have a fixed number Wc of logic «1»s per column and a fixed number Wr of logic «1»s per row. The second is the case of the irregular matrices whose number of logic «1»s per row is Wr and per column Wc , with $Wr \neq Wc$. The matrix is constituted by elements with values «0» and «1», and is sparse since most of the elements are null [26]. This matrix is described in equation (9).

$$H_{LDPC} = [A|B] \quad (9)$$

Matrix A has dimension $D \times E$ and matrix B is of dimension $D \times D$, where E corresponds to the number of information bits, D is the number of parity bits in

the LDPC codification, and $G = E + D$ would correspond to the length of the codeword. The regular LDPC matrices are divided in Gallager, characterized by a structure of horizontal bands [27], and in Mackay-Neal, characterized by a random construction [28]. These type of matrices do not guarantee the independence between columns required by the IRP in CS, thus they will not be used in this implementation [13].

The irregular matrices are divided in staircase and triangle [29]. They are matrices that contain two submatrices, and each of them uses a different method of creation [29, 30]. The left submatrix H_i of size $D \times E$ is constructed as follows:

- Use a vector which contains a random list of possible positions with «1»s in the rows. This vector is utilized to guarantee a homogeneous distribution.
- Place in each column Wc nonzero elements, choosing the positions of the vector of possible localizations. If the condition of a maximum number Wr of nonzero elements per row is not fulfilled now, choose another available random position.
- Add nonzero elements in the rows with less than two elements, to avoid decoding problems.

The right submatrix makes the difference in the formation of an irregular LDPC matrix, since it can be formed in staircase or in triangular shape, and in any case is a matrix of dimension $D \times D$. In the case of matrix Sc , it is an identity matrix in which nonzero elements are later placed in the lower diagonal part. Equation (10) shows a matrix H_{LDPC} constructed using this method.

$$(H_i|SC) = \begin{bmatrix} 0 & 1 & 0 & 1 & 1 & 1 & \vdots & 1 & 0 & 0 & 0 & 0 \\ 1 & 1 & 1 & 0 & 0 & 1 & \vdots & 1 & 1 & 0 & 0 & 0 \\ 1 & 0 & 1 & 1 & 1 & 0 & \vdots & 0 & 1 & 1 & 0 & 0 \\ 1 & 1 & 0 & 0 & 1 & 0 & \vdots & 0 & 0 & 1 & 1 & 0 \\ 0 & 0 & 1 & 1 & 0 & 1 & \vdots & 0 & 0 & 0 & 1 & 1 \end{bmatrix} \quad (10)$$

The right triangle submatrix Tr is constituted by an identity matrix of dimension $D \times D$ as base, and a sparse triangular lower matrix placed later. Equation (11) shows a H_{LDPC} matrix constructed by means of this method.

$$(H_i|Tr) = \begin{bmatrix} 0 & 1 & 0 & 1 & 1 & 1 & \vdots & 1 & 0 & 0 & 0 & 0 \\ 1 & 1 & 1 & 0 & 0 & 1 & \vdots & 1 & 1 & 0 & 0 & 0 \\ 1 & 0 & 1 & 1 & 1 & 0 & \vdots & 1 & 1 & 1 & 0 & 0 \\ 1 & 1 & 0 & 0 & 1 & 0 & \vdots & 1 & 0 & 1 & 1 & 0 \\ 0 & 0 & 1 & 1 & 0 & 1 & \vdots & 0 & 1 & 1 & 1 & 1 \end{bmatrix} \quad (11)$$

3. Implementation of CS and LDPC for channel estimation

This work is implemented in universal software radio peripheral (USRP) equipment. The block diagram of the implemented system is shown in Figure 2, where each stage of the communication system is presented.

The equipment used are the USRP Ettus X310, equivalent to the NI-USRP 2940R with the following specifications:

- Bandwidth up to 40 MHz per channel (2 channels).
- The image loaded in the FPGA enables a 1 Gbps Ethernet connection for 25 MS/s Full Duplex transmission.
- The used UHD architecture is the available for the «LABVIEW Communication Design Suite».
- Flexible clock architecture with configurable sampling frequency.

The bandwidth of the system is a function of the utilized IQ index, which determines the available bandwidth [31].

It should be indicated that with the purpose of working with a communication system closer to reality, a LDPC channel encoder has been used considering what was worked in [32, 33]. The selection of the H_{LDPC} matrices of this implementation was established by validation through the analysis of the BER. The selection of the matrix H_{LDPC} applied simulations with a varying sparsity of «1»s of the matrix considering an AWGN channel with Rayleigh fading. These matrices have a size of $G=40$ and $E=20$, due to their efficiency and velocity according to Figure 3. For this reason, the implementation of the channel encoder uses parity check matrices of staircase type.

3.2. Channel estimation with CS and LDPC

As indicated in section 2, the sensing matrix Φ should fulfill the IRP criterion to be able to appropriately recover the sparse signal; however, the matrix used in equation (13) fulfills this criterion at the restriction limits, since it is not random. Therefore, it is developed a matrix Φ_{LDPC} of pilot positions that improves this requirement. In a form similar to equation (13), each nonzero element corresponds to a position of each subpilot carrier in equation (15) [6].

$$\Phi_{LDPC} = \begin{bmatrix} \overbrace{1 \ 0 \ 0 \ 0 \ 0 \ 0 \ \dots \ 0 \ 0}^{N_f} \\ 0 \ 0 \ 0 \ 1 \ 0 \ 0 \ \dots \ 0 \ 0 \\ 0 \ 0 \ 0 \ 0 \ 0 \ 1 \ \dots \ 0 \ 0 \\ \vdots \ \vdots \ \vdots \ \vdots \ \vdots \ \vdots \ \ddots \ \vdots \ \vdots \\ 0 \ 0 \ 0 \ 0 \ 0 \ 0 \ \dots \ 0 \ 0 \end{bmatrix}_{P,N} \quad (15)$$

Equation (15) maintains the distance between the pilot subcarriers N_f as variable and pseudorandom, due to the use of the LDPC algorithms with which matrix H_{LDPC} is constructed. For the design of H_{LDPC} , the number of «1»s per row is equal to 1, taking into account the number of pilot subcarriers. In addition, the total percentage of nonzero elements should be equal to the number of pilots P .

After obtaining matrix Φ_{LDPC} , the process continues with the estimation of the channel, using the sparse reconstruction algorithms OMP and CoSaMP, considering the distribution of pilots obtained in Φ_{LDPC} .

3.3. Implemented scenarios

This work applied different scenarios, keeping a focus for Long Term Evolution (LTE) systems. For this purpose, characteristics of LTE indicated in [31,34] such as number of subcarriers, reference symbols, null subcarriers and length of the CP, were taken into account. A separation of 7.5 KHz between subcarriers was used, since the performance decays with the prolonged use of 15 KHz. Then, the implemented bandwidth was 1.92 MHz. It is necessary to clarify that a greater number of subcarriers was not used, as it is allowed by LTE, because the processing of the source code was carried out from the computer, and not on the FPGA of the equipment.

The first scenario implemented does not use the channel encoder and has the following characteristics:

- IQ sample rate: 1.92 MS/s.
- Frequency of carrier: 1.99 GHz.
- Modulation: 4 QAM.
- Iterations of the OMP algorithm: 5.

- Length of the transmitted message (bits train): 1600.
- Number of samples in the receiver: $3 \times$ total of transmitted data.
- Total number of OFDM subcarriers: 256.
- Total of subcarriers with data + pilot subcarriers: 150.
- Gain of the transmitter: 15.5 - 21 dB.
- Sensitivity of the receiver: 0 dB.

In order to obtain the results of the behavior of the channel estimators for the different sparse reconstruction algorithms, OMP and CoSaMP, as well as of the linear estimator, two separate SDR located in the test laboratory (indoor) at a considerable distance, as shown in Figure 2, were used. The distance was considered as constant, and the power of the equipment were modified to obtain variations of the signal to noise ratio (SNR), and subject the different channel estimators to the BER analysis.

For the second scenario the previous conditions were repeated, adding the LDPC channel encoder using the following configuration:

- Iterations of the propagation algorithm for the LDPC decoding: 100.
- Matrix H_{LDPC} with G=40 and E=20.
- Type of LDPC matrix in the encoder: staircase with sparsity of «1»s between 5 and 10%.

The final scenario of analysis is implemented with variable distance between transmitter and receiver, also in a closed environment to evaluate the channel in more rigorous conditions. The distance of separation between the SDRs considered the length, the physical distribution of the laboratory with distances between 4 and 10 meters, and a constant power which does not saturate the channel.

The variation of distance enabled to recreate channels with great fading, generating an increase of the multipath effect to evaluate the behavior of the estimators. The frequency of transmission is 2.4 Ghz, thus coexisting with the Wi-Fi network of the laboratory; this causes a continuous variation in the channel.

This scenario was worked in the presence of students, using an LDPC encoder with the following configuration:

- IQ sample rate: 1.92 MS/s.
- Frequency of carrier: 2.4 GHz.
- Modulation: 4 QAM.
- Iterations of the OMP algorithm: 5.

- Iterations of the propagation algorithm for the LDPC decoding: 100.
- Matrix H_{LDPC} with $G=40$ and $E=20$.
- Length of the transmitted message (bits train): 1240.
- Number of samples in the receiver: $2 \times$ total of transmitted data.
- Total number of OFDM subcarriers: 256.
- Total of subcarriers with data + pilot subcarriers: 150.
- Type of LDPC matrix in the encoder: staircase with sparsity of «1»s between 5 and 10%, 10 and 20% and 20 and 30%.
- Gain of the transmitter: 20 dB.
- Sensitivity of the receiver: 20 dB.

4. Analysis of the results

4.1. Scenarios 1 and 2 – BER Analysis

In the implementation of the OMP algorithm, the number of iterations should be chosen such that K corresponds to the number of nonzero elements of the signal to be recovered. In order to define this value, multiple tests were conducted seeking to minimize the error in the estimation of the channel, obtaining that the appropriate value for this algorithm to converge is $K = 5$, corresponding to the minimum number of subcarriers used.

Figure 4 shows the behavior of the BER with 5 and 25 pilot subcarriers, for the estimators based on OMP, CoSaMP and the linear estimator for the first scenario.

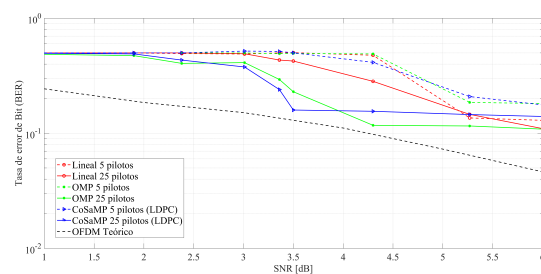


Figure 4. BER analysis without channel encoder.

It can be observed in Figure 4 that at low levels of SNR, the linear estimator exhibits a lower performance with respect to the employed estimators based on the CS paradigm. With 25 pilot subcarriers, the channel estimators achieve a considerable reduction in the probability of bits loss. In these tests, the algorithms CoSaMP and OMP worked with the Φ_{LDPC}

matrix and in its absence (comb-type pilot subcarriers distribution).

Figure 5 shows the behavior of the BER for 5 channel estimators, using the configurations of the second scenario. Then, according to what is expected with the use of a channel encoder, it can be observed in Figure 5(a) a clear improvement with respect to the previous case. The linear estimator exhibits the worst results for a low SNR. On the other hand, the CoSaMP estimators have a similar performance using matrix Φ_{LDPC} or not using it. However, the version with matrix Φ_{LDPC} exhibits a better performance. Also, as the SNR improves, the CoSaMP estimator without matrix Φ_{LDPC} has a slight improvement, but both continuing with the same trend in their behavior. On the other hand, the OMP estimators exhibit a lower performance compared with the CoSaMP, taking into account that the version with matrix Φ_{LDPC} is the one that offers the worst results for this particular algorithm.

Figure 5(b) shows the results of the performance of the estimators regarding the BER, using 25 pilot subcarriers for each of them. It can be observed that the linear estimator has the greatest probability of bit error for a low SNR, showing the worst performance among the estimators analyzed. Nevertheless, when the SNR a priori exceeds the value of 3.5 dB its performance improves, obtaining the smallest probability of bit error compared to the other estimators.

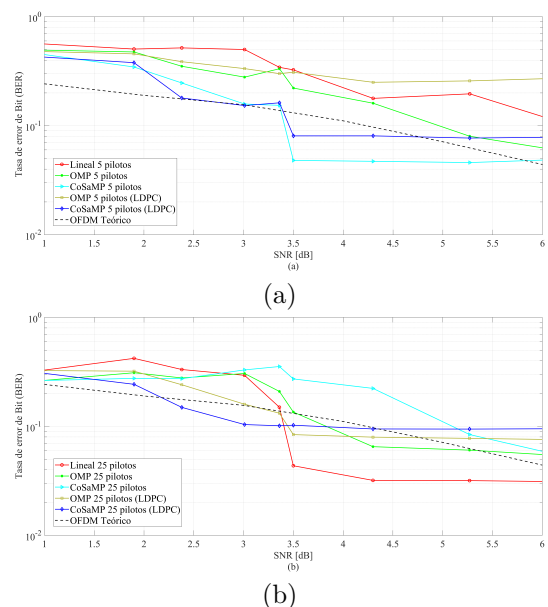


Figure 5. BER analysis with LDPC channel encoder: (a) BER with 5 pilots (b) BER with 25 pilots.

4.2. Scenario 3 - Analysis for variable distances

Figures 6 and 7 correspond to the behavior of the linear estimator, and of the estimators based on CS with and without matrix Φ_{LDPC} .

Figure 6 shows that the linear estimator has a better performance at a very short distance, which corresponds with the previous results in BER analysis. Nevertheless, as the distance increases, the performance of this channel estimator is drastically reduced. The CoSaMP estimator with Φ_{LDPC} is better compared with the estimator that uses OMP. It should be indicated that this figure takes into account the results using from 5 to 25 pilot subcarriers.

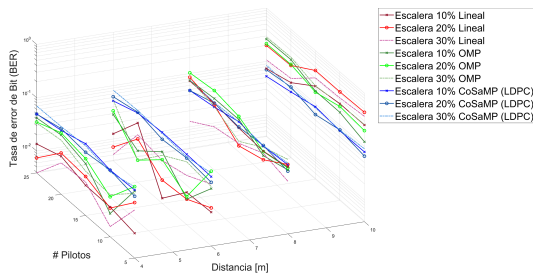


Figure 6. BER Analysis for different distances.

Since the channel decoder uses as input the responses of the channel estimators, the percentage of values that such decoder could not resolve was analyzed in this scenario. In this way, Figure 7 shows the percentage of null values (NaN) in contrast with the distance variations for each channel estimator.

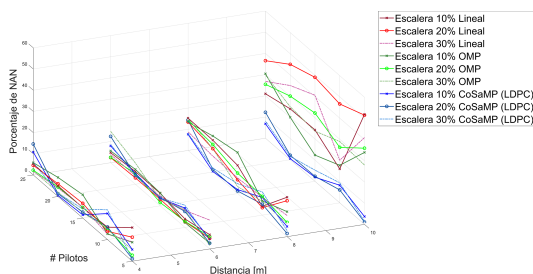


Figure 7. Analysis of the convergence of the channel decoder according to the response of the estimators at different distances.

Figure 7 also confirms the previous results, remarking the same trend in the estimators. The linear estimator works better at short distances, and the CS estimators have better performance than the linear ones for noisy channels, which is verified when the distance is increased.

4.3. Analysis of the bandwidth

Figure 8 shows the relationship between the bandwidth used by the pilot subcarriers and the bandwidth for sending information in an OFDM symbol. In this way,

using 5 pilot subcarriers instead of 25 corresponds to an improvement of 13.33% in spectral efficiency. This improvement corresponds to the use of the channel estimators based on CS, as seen in Figure 8.

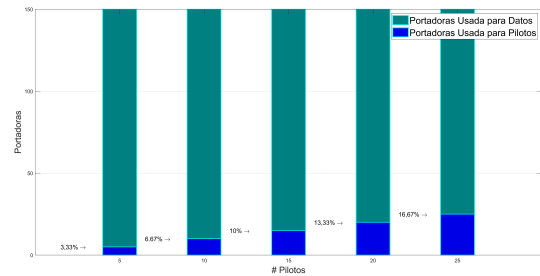


Figure 8. Bandwidth occupied at different number of pilots.

5. Conclusions

According to the results obtained, the CoSaMP estimators exhibit a better performance for low levels of SNR with the use of matrix Φ_{LDPC} . The OMP estimators show a behavior similar to the CoSaMP, even though with smaller performance. Thereby, with the results obtained it is deduced that, a linear estimator works with the channel estimation problem with very small computational complexity. Nevertheless, when the channel is very noisy, due mainly to the multipath, it demands more pilot subcarriers to try to maintain the performance, which reduces the effective bandwidth. In contrast, the estimators based on CS used in this work, besides maintaining low computational complexity, show an adequate performance for noisy channels enabling data transfer in such channels, considering that an indoor environment was evaluated.

The use of the CS paradigm improves while the IRP and null space properties are guaranteed; in this case, the channel may be considered as sparse because the number of pilot subcarriers is sparse.

In addition, implementing a sensing matrix designed based on the concept of LDPC matrices has enabled to improve the performance of the estimators based on CS, and this improvement is clearer for the estimator that uses OMP. The CoSaMP estimator with Φ_{LDPC} showed to be the best estimator in this working situation together with the channel encoder used.

Among the future works, it will be considered to implement channel estimation and prior processing procedures in the FPGA device, to enable that the communication between the equipment and the data source can use a higher data transmission rate.

References

- [1] J. Sterba and D. Kocur, "Pilot symbol aided channel estimation for ofdm system in frequency selective rayleigh fading channel," in *2009 19th International Conference Radioelektronika*, April 2009, pp. 77–80. [Online]. Available: <https://doi.org/10.1109/RADIOELEK.2009.5158729>
- [2] C. Tzi-Dar and T. Pei-Yun, *OFDM Baseband Receiver Design OFDM Baseband Receiver Design for Wireless Communications*, J. W. . S. A. P. Ltd, Ed., 2007. [Online]. Available: <http://doi.org/10.1002/9780470822500>
- [3] M. R. Raghavendra, S. Bhashyam, and K. Giridhar, "Exploiting hopping pilots for parametric channel estimation in ofdm systems," *IEEE Signal Processing Letters*, vol. 12, no. 11, pp. 737–740, Nov 2005.
- [4] N. N. Jimenez Castro Martínez, "Identificación ciega de canal disperso basado en algoritmos de sub-espacio," Master's thesis, 2016. [Online]. Available: <http://inaoe.repositorioinstitucional.mx/jspui/handle/1009/40>
- [5] M. Cordero Limón, "Técnicas de estimación de canal en la capa física wirelessman-ofdm de la norma ieee 802.16e," 2009. [Online]. Available: <https://bit.ly/2P9Q1co>
- [6] S. Zhang, J. Kang, Y. Song, and N. Wang, "An optimization for channel estimation based on compressed channel sensing," in *2012 13th ACIS International Conference on Software Engineering, Artificial Intelligence, Networking and Parallel/Distributed Computing*, Aug 2012, pp. 597–602. [Online]. Available: <https://doi.org/10.1109/SNPD.2012.128>
- [7] Y. Liao, G. Sun, X. Shen, S. Zhang, X. Yang, X. Zhang, H. Yao, and N. Zhang, "Bem-based channel estimation and interpolation methods for doubly-selective ofdm channel," in *2018 IEEE International Conference on Smart Internet of Things (SmartIoT)*, Aug 2018, pp. 70–75. [Online]. Available: <https://doi.org/10.1109/SmartIoT.2018.00022>
- [8] Y. A. Al-Jawhar, K. N. Ramli, M. A. Taher, N. S. Mohd Shah, L. Audah, and M. S. Ahmed, "Zero-padding techniques in ofdm systems," *International Journal on Electrical Engineering and Informatics*, vol. 10, no. 4, pp. 704–725, 2018. [Online]. Available: <https://bit.ly/2YAQGqc>
- [9] P. H. Moose, "A technique for orthogonal frequency division multiplexing frequency offset correction," *IEEE Transactions on Communications*, vol. 42, no. 10, pp. 2908–2914, Oct 1994. [Online]. Available: <https://doi.org/10.1109/26.328961>
- [10] J. van de Beek, M. Sandell, and P. O. Börjesson, *ML estimation of timing and frequency offset in multicarrier systems*, div. of signal processing lulea university of technology s-971 87 lulea, sweden ed. Luleå tekniska universitet, 1996. [Online]. Available: <https://bit.ly/38qaO2W>
- [11] D. L. Donoho, "Compressed sensing," *IEEE Transactions on Information Theory*, vol. 52, no. 4, pp. 1289–1306, April 2006. [Online]. Available: <https://doi.org/10.1109/TIT.2006.871582>
- [12] R. G. Baraniuk, "Compressive sensing [lecture notes]," *IEEE Signal Processing Magazine*, vol. 24, no. 4, pp. 118–121, July 2007. [Online]. Available: <https://doi.org/10.1109/MSP.2007.4286571>
- [13] R. Baraniuk, M. A. Davenport, M. F. Duarte, and C. Hegde, *An introduction to compressive sensing*, 2011. [Online]. Available: <https://bit.ly/38uCOCG>
- [14] Milliarde. (2016) Compressed sensing intro & tutorial w/ matlab. CODE PROJECT for those who code. [Online]. Available: <https://bit.ly/2YC5Ewa>
- [15] J. Inga-Ortega, E. Inga-Ortega, C. Gómez, and R. Hincapié, "Electrical load curve reconstruction required for demand response using compressed sensing techniques," in *2017 IEEE PES Innovative Smart Grid Technologies Conference - Latin America (ISGT Latin America)*, Sep. 2017, pp. 1–6. [Online]. Available: <https://doi.org/10.1109/ISGT-LA.2017.8126731>
- [16] M. Pinos and J. Inga, "Predicción de consumo eléctrico en la UPS de Cuenca usando P1P y censado comprimido," 2018.
- [17] E. J. Candes and M. B. Wakin, "An introduction to compressive sampling," *IEEE Signal Processing Magazine*, vol. 25, no. 2, pp. 21–30, March 2008. [Online]. Available: <https://doi.org/10.1109/MSP.2007.914731>
- [18] E. J. Candés, "The restricted isometry property and its implications for compressed sensing," *Comptes Rendus Mathématique*, vol. 346, no. 9, pp. 589–592, 2008. [Online]. Available: <https://doi.org/10.1016/j.crma.2008.03.014>
- [19] E.-G. Astaiza-Hoyos and H. F. Pablo Emilio Bermúdez-Orozco, "Compressive sensing: A methodological approach to an efficient signal processing," *Dyna*, 2015. [Online]. Available: <https://bit.ly/2qLx8TI>

- [20] H. Yuan, H. Song, X. Sun, K. Guo, and Z. Ju, "Compressive sensing measurement matrix construction based on improved size compatible array ldpc code," *IET Image Processing*, vol. 9, no. 11, pp. 993–1001, 2015. [Online]. Available: <https://doi.org/10.1049/iet-ipr.2015.0117>
- [21] A. G. Dimakis, R. Smarandache, and P. O. Vontobel, "Ldpc codes for compressed sensing," *IEEE Transactions on Information Theory*, vol. 58, no. 5, pp. 3093–3114, May 2012. [Online]. Available: <https://doi.org/10.1109/TIT.2011.2181819>
- [22] S. Pawar and K. Ramchandran, "A hybrid dft-ldpc framework for fast, efficient and robust compressive sensing," in *2012 50th Annual Allerton Conference on Communication, Control, and Computing (Allerton)*, Oct 2012, pp. 1943–1950. [Online]. Available: <https://doi.org/10.1109/Allerton.2012.6483460>
- [23] H. Wang, W. Du, and Y. Bai, "Compressed sensing based channel estimation for OFDM transmission under 3 GPP channels," *International Journal of Future Generation Communication and Networking*, vol. 9, no. 4, pp. 85–94, 2016. [Online]. Available: <http://dx.doi.org/10.14257/ijfgcn.2016.9.4.08>
- [24] D. Needell and J. A. Tropp, "Cosamp: Iterative signal recovery from incomplete and inaccurate samples," *Applied and Computational Harmonic Analysis*, vol. 26, no. 3, pp. 301–321, 2009. [Online]. Available: <https://doi.org/10.1016/j.acha.2008.07.002>
- [25] B. L. Sturn. (2011) Algorithm power hour: Compressive sampling matching pursuit (cosamp). [Online]. Available: <https://bit.ly/2RS0DOX>
- [26] I. D. F. Lava, "Implementación y evaluación de la codificación ldpc para la transmisión de ficheros en entornos unidireccionales," in *Computer Science*, 2013. [Online]. Available: <https://bit.ly/2YCauJQ>
- [27] R. Gallager, "Low-density parity-check codes," *IRE Transactions on Information Theory*, vol. 8, no. 1, pp. 21–28, January 1962. [Online]. Available: <https://doi.org/10.1109/TIT.1962.1057683>
- [28] D. J. C. Mackay, *Information Theory, Inference and Learning Algorithms*. Cambridge University Press, 2003. [Online]. Available: <https://bit.ly/2E5yfQX>
- [29] G. G. Andrade Salinas, "Implementación de la codificación y decodificación del código LDPC (low density parity check) en MATLAB," 2017. [Online]. Available: <https://bit.ly/34ahKxG>
- [30] V. Roca, C. Neumann, and D. Furodet. (2008) Low density parity check (ldpc) staircase and triangle forward error correction (fec) schemes. [Online]. Available: <https://bit.ly/2RH8PBq>
- [31] E. Seidel, "Overview lte phy: Part 1 - principles and numerology etc," *NOMOR Research*, 2007. [Online]. Available: <https://bit.ly/35cxH7R>
- [32] R. Prieto, A. Abril, and A. Ortega, "Experimental alamouti-stbc using ldpc codes for mimo channels over sdr systems," in *2017 IEEE 30th Canadian Conference on Electrical and Computer Engineering (CCECE)*, April 2017, pp. 1–5. [Online]. Available: <https://doi.org/10.1109/CCECE.2017.7946842>
- [33] B. Peñafiel and A. Ortega, "A joint multilevel modulator and robust ldpc codes processing over optical systems by providing solutions for holistic 5g backhaul," in *2017 IEEE 13th Malaysia International Conference on Communications (MICC)*, Nov 2017, pp. 197–202. [Online]. Available: <https://doi.org/10.1109/MICC.2017.8311758>
- [34] J. Zyren, "Overview of the 3gpp long term evolution physical layer," NXP Semiconductors, Tech. Rep., 2007. [Online]. Available: <https://bit.ly/35gg8E0>